15TH IEA HEAT PUMP CONFERENCE
MAY 26–29, 2026 | HOFBURG
VIENNA 2026
DECARBONISATION THROUGH INNOVATION

Comparative Assessment of the Thermodynamic Performance and Application Area of Mechanical Vapor Compression and Joule Brayton High Temperature Heat Pumps

Maja Sharevska[a,*], Monika Sharevska[a], Gerrit Brem[a], Gerwin Hoogsteen[b,c], Johann Hurink[b], Artur Pozarlik[a], Yashar Hajimolana[a]

[a]Department of Thermal and Fluid Engineering, Faculty of Engineering Technology, University of Twente, The Netherlands
[b]Department of Applied Mathematics, Faculty of Electrical Engineering, Mathematics and Computer Science, University of Twente, The Netherlands
[c]Department of Computer Science, Faculty of Electrical Engineering, Mathematics and Computer Science, University of Twente, The Netherlands

Abstract

High-temperature heat pumps (HTHPs) providing heat at up to 150°C are already available and can be used to decarbonize a large share of industrial heat demand. Increasing the temperature that HTHPs can deliver will allow for an increase in this share further. However, for reaching temperatures higher than the critical temperature of most refrigerants, the conventional closed refrigeration vapor-compression thermodynamic cycle working with traditional refrigerants is no longer a feasible option. This paper investigates and compares two promising cycles for delivering heat above 150°C: open cycle mechanical vapor compression (MVC) (R718) HTHP and Joule-Brayton (R729, R740, R744) HTHP. Hereby, centrifugal compressors and turboexpanders are considered. Thermodynamic models of the proposed HTHPs are developed with a CoolProp interface. These models are used to study the thermodynamic performance of the MVC and the Joule-Brayton HTHP, including the COP, maximum temperature, and required compressor pressure ratio and peripheral speed. The three-stage MVC HTHP achieves condensation temperatures of up to 350°C with high superheating at the compressor outlet of 500°C. Moreover, the MVC has a high COP (2-10) for large temperature lift (160-30 K). The Joule-Brayton HTHP generates high-temperature heat (150-500°C) with a reasonable COP (2.2-1.35). Based on the results, guidelines for selecting a HTHP are given with regards to the characteristics of the waste heat carrier and the process heat carrier. The MVC HTHP is recommended for steam generation and applications when the waste heat source is low pressure steam. The Joule-Brayton HTHP is recommended if sensible heat is required with a large temperature rise of the process heat carrier and a large temperature drop of the waste heat carrier. Finally, the study indicates the application area where MVC and Joule-Brayton HTHP can decarbonize process heat demand at up to 500°C.

Selection and/or peer-review under the responsibility of the organizers of the 15th IEA Heat Pump Conference 2026.

Keywords: High-temperature heat pump; R718 mechanical vapor compression; Joule-Brayton; COP; Centrifugal compressor.

1. Introduction

Process heat accounts for the largest share of energy consumption in the industry, and a substantial portion of this demand is required at temperatures below 500°C. High-temperature heat pumps (HTHPs) that provide heat up to 150°C are increasingly adopted as an industrial decarbonization technology. One of the main perspectives for HTHP research is to increase the delivered temperature further [1]. However, for temperatures above the critical temperature of most refrigerants, the conventional closed vapor-compression refrigeration (heat pump) cycle with traditional refrigerants is no longer a feasible option. To overcome this limitation, two cycle concepts have emerged as promising technologies: the R718 open-cycle mechanical vapor compression

*Corresponding author. *E-mail address: m.sharevska@utwente.nl*

(MVC) HTHP [2] and the Joule-Brayton HTHP [3,4] using superheated refrigerants such as R729 (air), R740 (argon), and R744 (carbon dioxide). The high critical temperature of R718 enables operation at significantly elevated discharge temperatures. In the reversed Joule-Brayton cycle (referred to as Joule-Brayton in the remainder of the text), the refrigerant remains in the superheated gas region throughout the process, allowing for high-temperature heat delivery without phase change. A comprehensive overview of HTHP studies can be found in our previous work [5,6].

This paper aims to compare the thermodynamic performance and application potential of these two concepts by developing thermodynamic models implemented in MATLAB with CoolProp interface and comparing their performance across a wide temperature range. The study evaluates the achievable temperature lift, COP, volumetric heating capacity, and required compressor pressure ratio and peripheral speed, and provides guidance for selecting an appropriate HTHP cycle.

2. Methodology

This section presents the methodology to study the thermodynamic performance of the R718 open-cycle MVC HTHP and the Joule-Brayton HTHP. The following modeling assumptions are made:

- Steady state conditions in the HTHP components.
- Pressure drops in the heat exchangers are neglected.
- Saturated vapor at the compressor inlet and saturated liquid at the condenser exit.
- Adiabatic operation of the compressor.
- Centrifugal compressor isentropic efficiency of 80 %.
- Turboexpander isentropic efficiency of 85 %.

The compressor pressure ratio is determined by the peripheral speed. For a given peripheral speed and for different compressor inlet temperatures T_1, the compressor pressure ratio (Π) is calculated according to Eq. (1) [7], where ψ=0.7 is the work coefficient, η_P=0.82 is the compressor polytropic efficiency, and κ is the isentropic exponent at temperature T_1.

$$\Pi = \left(1 + \psi(\kappa - 1)\frac{M_u^2}{\eta_p}\right)^{\frac{\kappa}{\kappa-1}\eta_p} \tag{1}$$

High impeller peripheral speeds (u_2) of 600-700 ms^{-1} have been achieved [8,9]. Hence, the maximum achievable pressure ratio is obtained for peripheral Mach number (M_u=u_2/a_1) corresponding to u_2=700 ms^{-1} and local speed of sound (a_1) at a given compressor inlet temperature. Additionally, the fluid flow Mach number (M_{w1}) must not exceed 1 [10,11]. This is especially important when the molecular mass of the refrigerant is higher, because a high Mach number appears at a relatively small peripheral speed. Generally, a peripheral Mach number (M_u) lower than 1.5 has been considered safe for operation [5–7].

The achievable temperature lift at different evaporation (compressor inlet) temperatures for R718 MVC single-stage compressor is given by Eq. (2), where the maximum achievable condensation temperature is given as the saturation temperature corresponding to the pressure (p_{cmaxi} =$\Pi_{max}\, p_{ei}$).

$$\Delta T_{\max i} = T_{c\,max} - T_{e\,i} = T_{sat}|_{\Pi_{max} p_{e\,i}} - T_{sat}|_{p_{e\,i}} \tag{2}$$

The achievable compressor temperature lift at different compressor inlet temperatures for R729, R740, and R744 Joule-Brayton single-stage compressors is given by Eq. (3), where the maximum achievable compressor outlet temperature is given as the temperature corresponding to the pressure (p_{2maxi} =$\Pi_{max}\, p_{1i}$).

$$\Delta T_{\max i} = T_{2\,max} - T_{1\,i} = T_2|_{\Pi_{max} p_{1\,i}} - T_{1\,i} \tag{3}$$

The thermodynamic states of MVC HTHP cycle are defined according to Figure 1. The maximum achievable temperature with three-stage MVC is calculated for the maximum pressure ratio for each stage. Hereby, the maximum pressure ratio for each stage, as given by Eq. (1), is evaluated for the conditions at the inlet of each stage. The outlet of each compression stage is determined using isentropic compression and isentropic efficiency.

$$h_2 = h_1 + \frac{1}{\eta_C}(h_{2s} - h_1)$$

$$h_4 = h_3 + \frac{1}{\eta_C}(h_{4s} - h_3)$$

$$h_6 = h_5 + \frac{1}{\eta_C}(h_{6s} - h_5)$$

The temperature at each compressor outlet is evaluated with CoolProp interface for known enthalpy and pressure.

The evaporated liquid for intercooling (x_{l1} from state 2 to state 3 and x_{l2} from state 4 to state 5) is considered when calculating the specific compression work of the second stage and third stage and the specific heating effect.

$$x_{l1} = \frac{h_2 - h_3}{h_3 - h_l|_{x_l=0,p_1}}$$

$$x_{l2} = \frac{h_4 - h_5}{h_5 - h_l|_{x_l=0,p_1}}$$

The maximum achievable condensation temperature is determined as the saturation temperature at the pressure achieved by the third stage. The heat generated during final desuperheating (q_{c1}), specific heating effect (q_{con}), specific heat for liquid water heating, specific compression work (l) in C1, C2, and C3, temperature at compressor outlet, COP, an adjusted COP are calculated according to Eqs. (4-9).

$$q_{c1} = (1 + x_{l1} + x_{l2})(h_6 - h_7) \tag{4}$$

$$q_{con} = (1 + x_{l1} + x_{l2})h_{fg}\big|_{p_c} + q_{c1} \tag{5}$$

$$q_{wh} = h_{7l} - h_{1l} \tag{6}$$

$$l_{c_1} = h_2 - h_1 \tag{7a}$$

$$l_{c_2} = (1 + x_{l1})(h_4 - h_3) \tag{7b}$$

$$l_{c_3} = (1 + x_{l1} + x_{l2})(h_6 - h_5) \tag{7c}$$

$$COP = \frac{q_{con}}{l_{c_1} + l_{c_2} + l_{c_3}} \tag{8}$$

$$COP_{adj} = \frac{q_{con} + q_{wh}}{l_{c_1} + l_{c_2} + l_{c_3}} \tag{9}$$

The thermodynamic states of a regenerative Joule Brayton HTHP cycle are defined according to Figure 2. The specific heating effect due to refrigerant cooling from state 2 to state 3, specific compression work, specific expansion work, and COP are calculated according to Eqs. (10-13). For the regenerator, a pinch temperature difference of 5 K is assumed.

$$q_{con} = h_2 - h_3 \tag{10}$$

$$l_C = h_2 - h_1 \tag{11}$$

$$l_E = h_4 - h_5 \tag{12}$$

$$COP = \frac{q_{con}}{l_C - l_E} \tag{13}$$

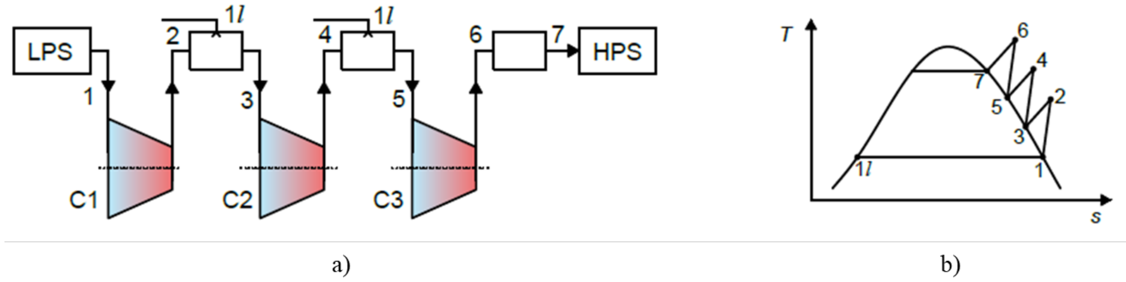

Figure 1 Schematic diagram (a) and temperature-entropy diagram (b) of MVC HTHP

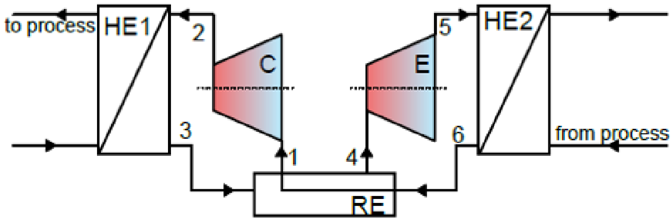

a)

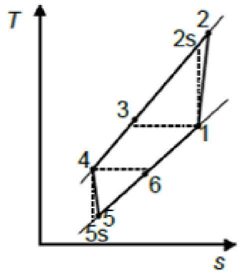

b)

Figure 2 Schematic diagram (a) and temperature-entropy diagram (b) of Joule-Brayton HTHP

3. Results

This section presents the results from the methodology for the centrifugal compressors' application in HTHPs and the thermodynamic performance of MVC and Joule-Brayton HTHPs. Based on this, guidance for selecting an appropriate HTHP is provided.

3.1. Centrifugal compressors

For R718 centrifugal compressors, the primary design constraint is the impeller peripheral speed. Figure 3 presents the relationship between temperature lift, pressure ratio, and peripheral speed. The maximum achievable pressure ratio is indicated with dotted lines for four different peripheral speeds: 400, 500, 600, and 700 ms^{-1}. At lower evaporation temperatures, the maximum pressure ratio decreases as the inlet temperature increases, which can be attributed to the rise in local speed of sound (Figure 4) and the resulting reduction in peripheral Mach number (shown in Figure 5) for fixed peripheral speed limit. Once the evaporation temperature exceeds approximately 200°C, the trend reverses and the maximum pressure ratio begins to increase. Two factors contribute to this behavior: the isentropic exponent increase and the compressibility factor drop, which determine the local speed of sound (Figure 4).

The achievable temperature lift increases with the evaporation temperature and at elevated inlet temperatures such as 260°C, a single stage centrifugal compressor can deliver temperature lifts up to 110 K. This is an important capability for MVC HTHPs targeting heat delivery at around 350°C. Comparable operational limits were also noted by Bergamini et al. [12] for a two-stage centrifugal compressors with a pressure ratio of 22.1.

For R729, R740, and R744 centrifugal compressors (applied in Joule-Brayton HTHPs), Figure 6 shows the relationship between the compressor temperature lift (T_2-T_1), pressure ratio, and the impeller peripheral speed. Due to R740's higher molecular mass compared to R729, it achieves higher pressure ratios for the same peripheral speed. Moreover, its thermodynamic properties give possibilities for higher temperature lifts for a given pressure ratio. The highest molecular mass of R744 results in the highest achievable pressure ratio for the same limits in peripheral impeller speed. However, special attention should be paid to the limitations of the fluid flow Mach number (M_{w1}). Peripheral Mach numbers higher than 1.5 and corresponding pressure ratio higher than 6 need additional effort when designing the impeller to ensure the fluid flow Mach number is less than 1 [10,11,13].

The presented relationships illustrate the strong coupling between turbomachinery operating limits and the maximum deliverable heat temperature in HTHPs.

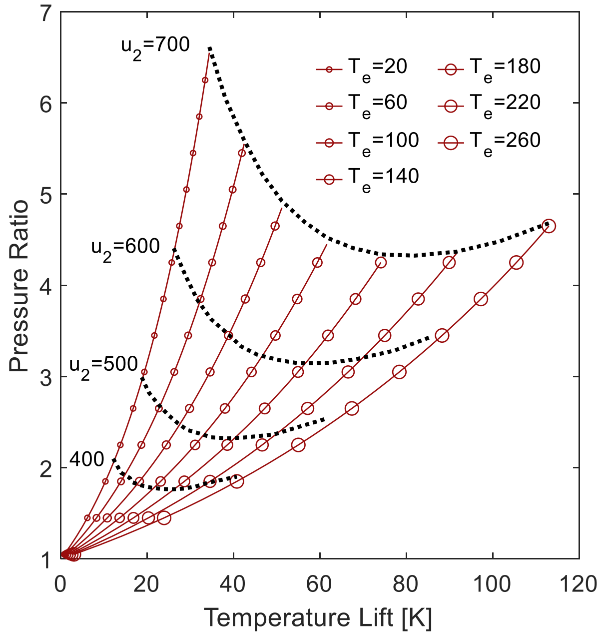

Figure 3 Required pressure ratio and peripheral speed dependence on temperature lift for different compressor inlet temperatures for R718

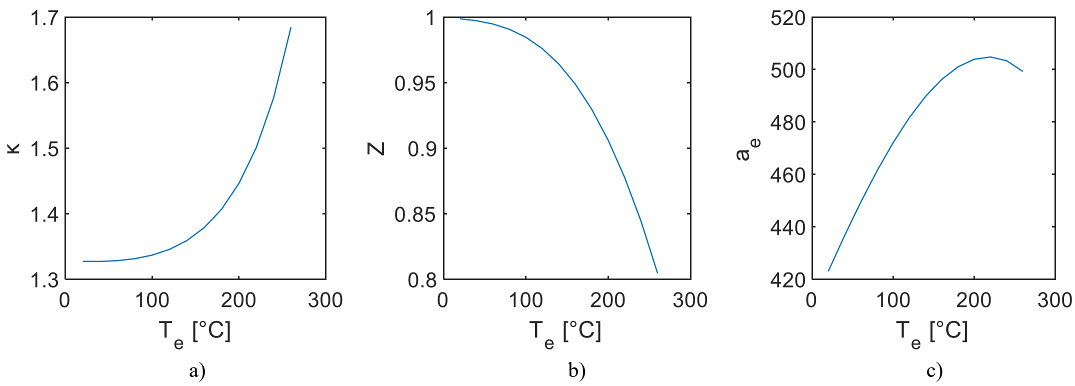

Figure 4 Thermodynamic properties of R718 a) isentropic exponent, b) compressibility factor, c) local speed of sound

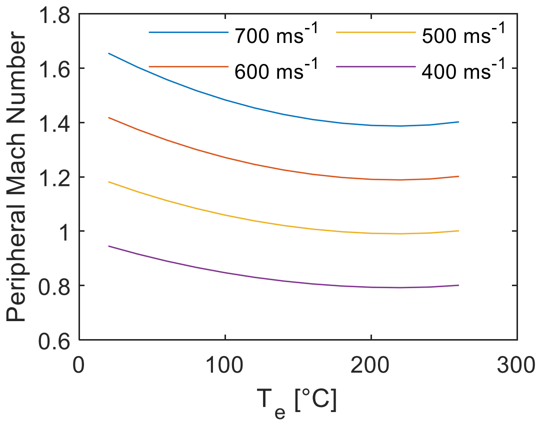

Figure 5 Peripheral Mach number for R718 centrifugal compressor at different inlet temperatures and impeller peripheral speeds

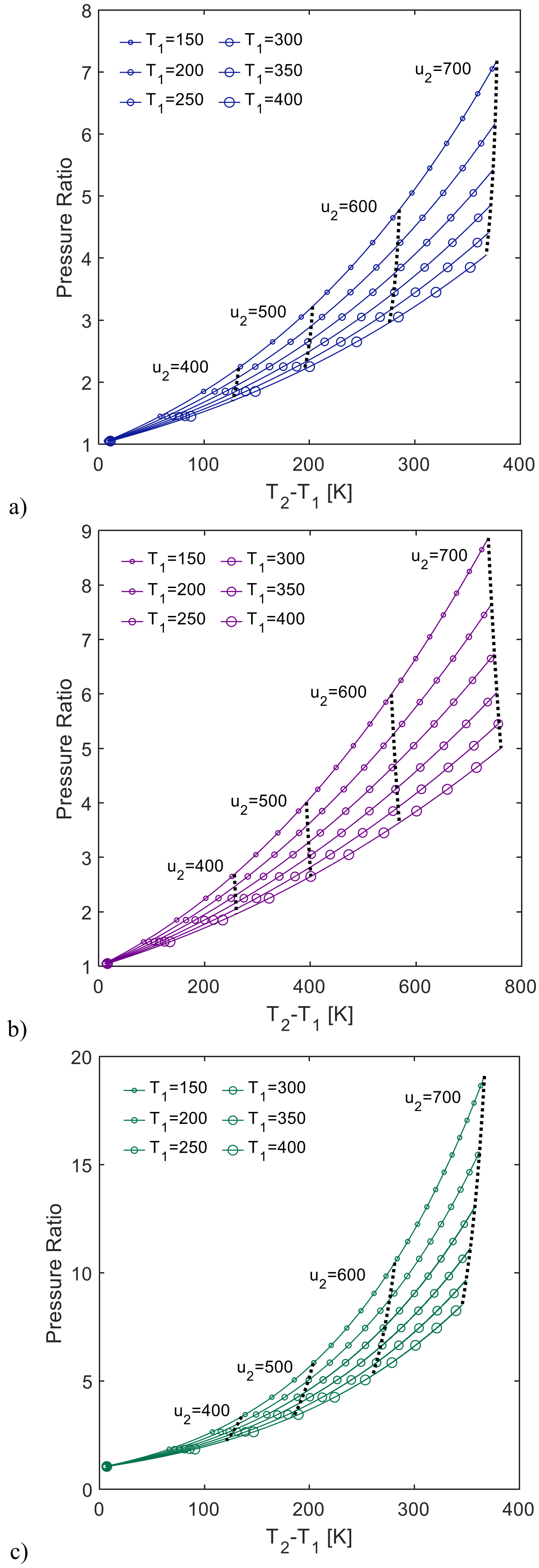

Figure 6 Required pressure ratio and peripheral speed dependence on compressor temperature lift for different compressor inlet temperatures for a) R729, b) R740, and c) R744

3.2. R718 mechanical vapor compression HTHP

Figure 7 shows the maximum condensation temperature achievable with a three-stage MVC for different limitations of the centrifugal compressor peripheral speed and the corresponding COP. According to Section 3.1. the possible temperature lift increases with evaporation temperature. Consequently, high condensation temperature of 360 °C is possible for high evaporation temperature of 120 °C and 700 ms^{-1} peripheral speed, and condensation temperature of 280 °C for 600 ms^{-1} peripheral speed in Figure 7a. The larger lift achieved with 700 ms^{-1} peripheral speed is reflected in the lower COP of 1.3 for 700 ms^{-1} compared to 2.2 for 600 ms^{-1} in Figure 7b.

High superheating occurs for R718 as shown in Figure 8. For the saturation temperatures at each compressor stage outlet indicated in Figure 8a, superheating of above 130 K occurs. This is due to both the high pressure ratio and the high isentropic exponent of R718. For this reason, intercooling between stages is necessary [8].

However, such high superheating is beneficial in HTHP applications. Figure 9 shows the distribution of the delivered heat between the latent heat at condensation temperature and the heat from the final-stage desuperheating. For an evaporation temperature of 120°C, the condensation approaches the critical point and the latent heat of condensation decreases. At the same time, the heat from desuperheating (from 485°C to 360°C) increases and reaches a point where it equals the latent heat of condensation (Figure 9).

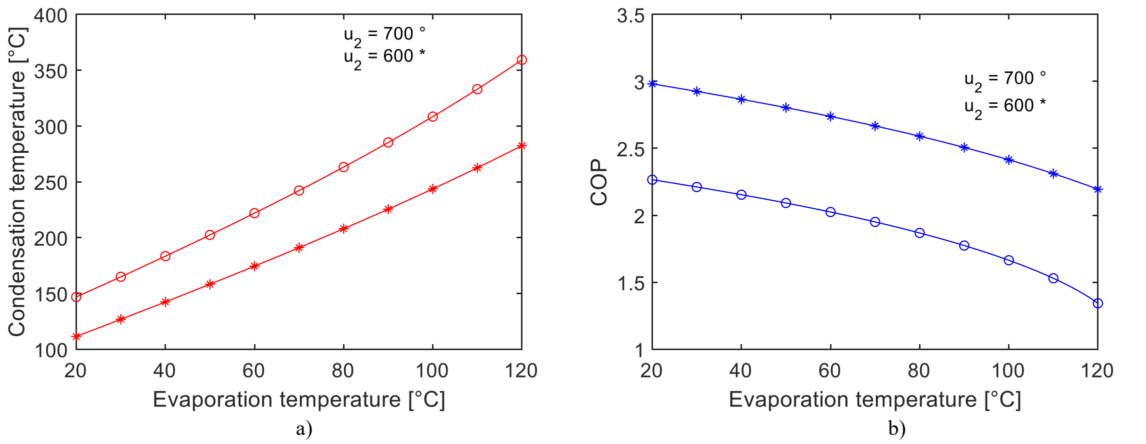

Figure 7 Maximum achievable condensation temperature (a) and the associated COP (b) for a three stage mechanical vapor compression system at different evaporation temperatures

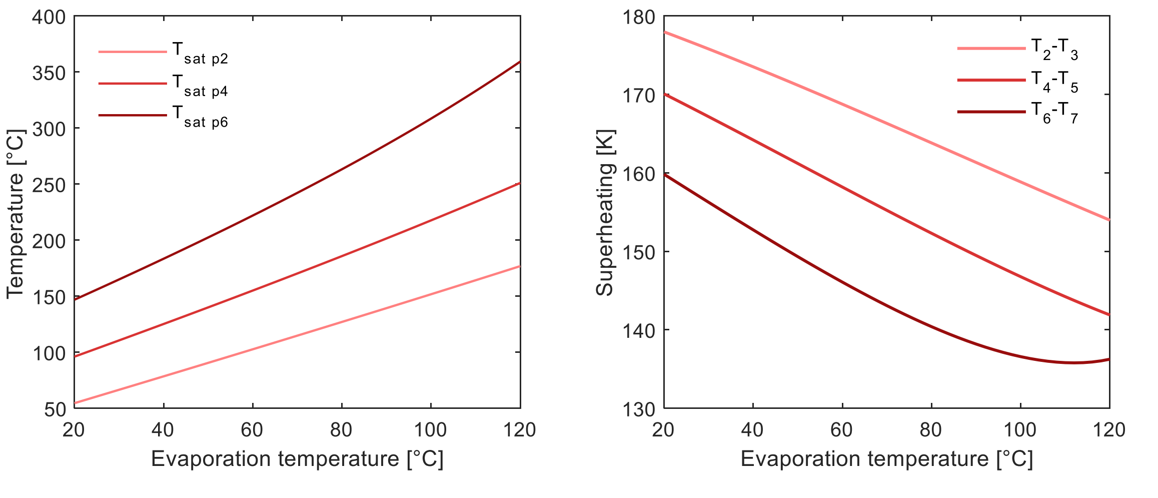

Figure 8 Saturation temperature at each compressor stage outlet (a) and superheating (b) at different evaporation temperatures for maximum achievable pressure ratio (u_2=700 ms^{-1})

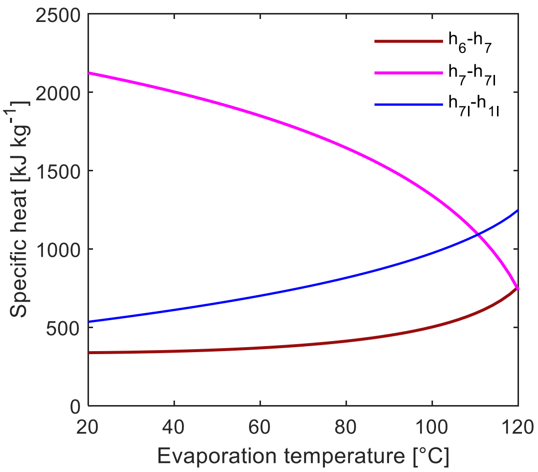

Figure 9 Latent heat at condensation temperature (h_7-h_{7l}), desuperheating from compressor outlet temperature (h_6-h_7), and water heating (h_{7l}-h_{1l}) for different evaporation temperatures

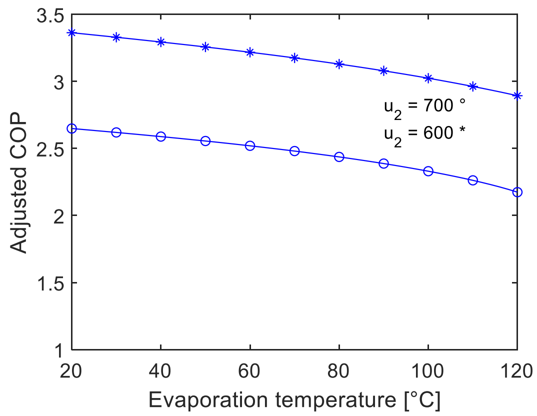

Figure 10 COP adjusted to account for the energy of water heating from evaporation temperature to condensation temperature

In addition, Figure 9 shows the heat required for liquid water heating from evaporation to condensation temperature. If the heat needed for liquid heating is considered, higher efficiencies can be declared. This adjusted COP is shown in Figure 10 and is more suitable for comparison of MVC to conventional steam boilers. The value of this adjusted COP for condensation temperature of 360 °C, evaporation temperature of 120 °C, and 700 ms^{-1} peripheral speed is 2.2, whereas for condensation temperature of 280 °C, evaporation temperature of 120 °C, and 600 ms^{-1} peripheral speed is 2.9.

The results presented here are for the highest achievable temperature lifts. However, when the MVC is applied for lower temperature lifts (30 K) COP of 10 is achieved [6].

MVC HTHPs are recommended for steam generation using industrial waste heat as an alternative to conventional steam boilers. Additionally, they are recommended for upgrading conventional closed-cycle HTHPs to further increase the delivered temperature. If the waste heat carrier is waste steam, it is directly used in the MVC. Otherwise, if the waste heat carrier is waste water, direct flash evaporation or a heat recovery steam generator can be applied before the MVC. In direct flash evaporation, the waste water is throttled to a two-phase state and the liquid and vapor phases are separated in a flash tank. The vapor fraction is the low-pressure steam which is further upgraded in the MVC. In a heat recovery steam generator, the heat from the waste water is recovered in a heat exchanger to produce low-pressure steam which is further upgraded in the MVC [6]. For all other waste heat carriers, low-pressure steam is generated in a heat recovery steam generator. For low-temperature waste heat a conventional closed-cycle heat pump can be implemented to generate low-pressure steam which is further upgraded using MVC [14]. The superheated steam generated by MVC serves as a process heat carrier.

3.3. Joule-Brayton HTHP

Figure 11 shows the influence of the temperature change in the R729 cooler (T_2-T_3) on the COP for different temperatures at the R729 heater exit (T_6). For T_3 fixed by the process heat carrier conditions, the requirements for T_2 are met by varying the pressure ratio. The pressure ratio corresponding to the requirements for T_2 is given in Figure 6a. As the required T_2 increases, the compressor must achieve higher pressure ratios. This pressure ratio increase initially has a slight positive effect on the COP, because more expansion work is recovered. However, it quickly reaches a maximum and any further increase in pressure ratio increases the compression work and hence the COP drops.

Similar COP values for the same conditions are achievable with R740, as shown in Figure 12. However, in this case, the required pressure ratios and the impeller peripheral speeds are lower (Figure 6b). This means that higher temperature lifts are achievable.

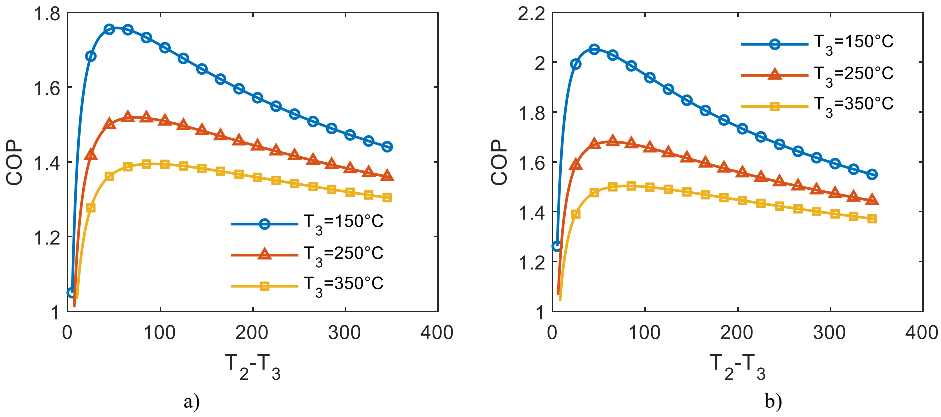

Figure 11 R729 Joule-Brayton HTHP COP dependence on the temperature change in the R729 cooler for outlet temperature of R729 heater of T_6=50°C (a) and T_6=100°C (b)

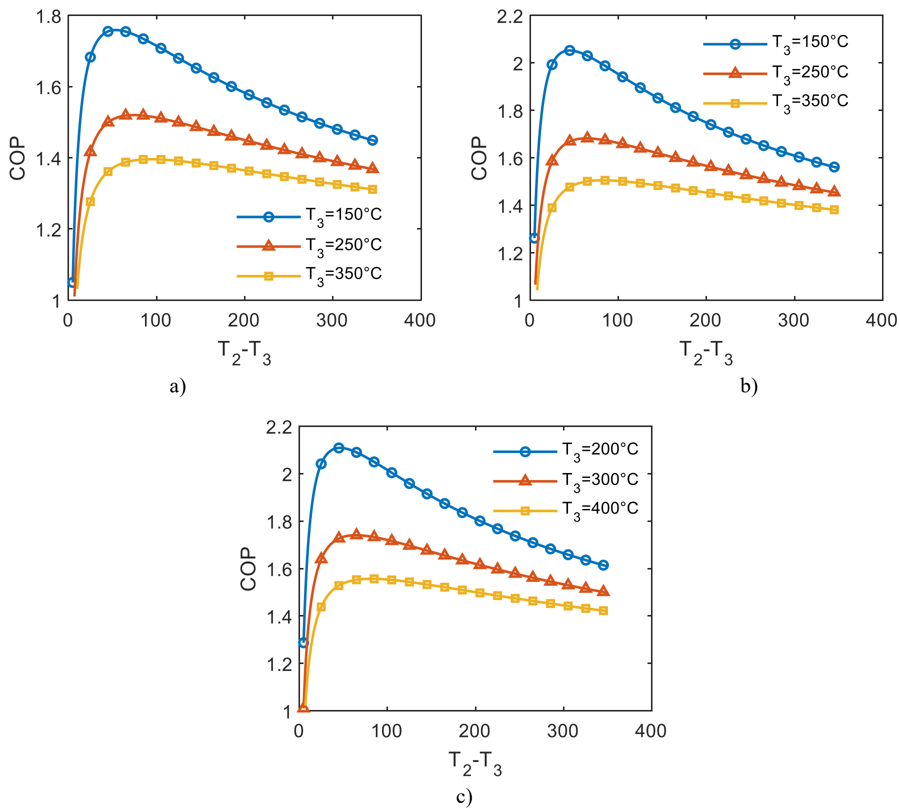

Figure 12 R740 Joule-Brayton HTHP COP dependence on the temperature change in the R740 cooler for outlet temperature of R740 heater of T_6=50°C (a), T_6=100°C (b), and T_6=150°C (c)

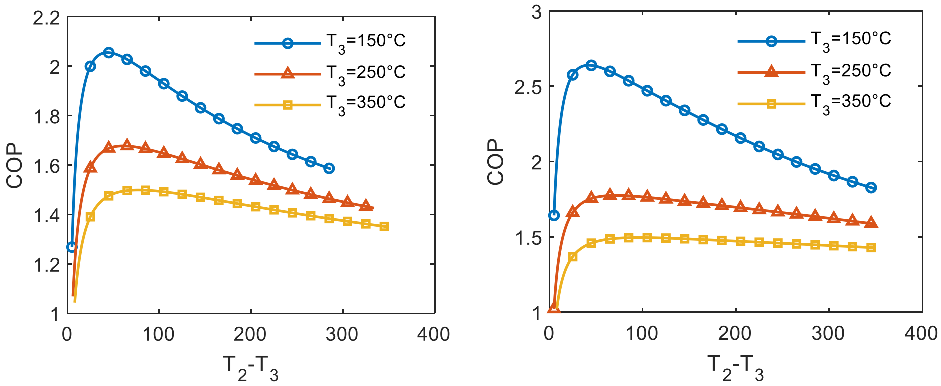

a) b)

Figure 13 R744 Joule-Brayton HTHP COP dependence on the temperature change in the R744 cooler for compressor inlet pressure of p_1=1 bar (a) and p_1=80 bar (b) (T_6=100°C)

Similar values for COP are also obtained for R744, as shown in Figure 13a. Higher COP can be obtained if the compressor inlet pressure is higher (p_1=80 bar, Figure 13b). However, in both cases, the higher temperature lifts are only possible with higher compression pressure ratios (Figure 6). In such conditions (temperature lift higher than 300 K), a two-stage compressor should be applied. Note that, in Figure 13a, for high temperature lifts and low temperatures at R744 cooler exit (T_3), the expander outlet state is in the two-phase region and therefore these results are removed.

Regenerative Joule-Brayton HTHPs are recommended for high temperature lifts and for high temperature differences (i.e., temperature glide) of the process heat carriers and waste heat carriers (usually air) along the heat exchangers. The temperature difference of hot air as a process heat carrier matches the temperature difference for R729 HTHP, whereas for other process heat carriers, a minimal pinch temperature difference (3 – 5 K) ensures effective heat transfer. Though the COP is relatively low, they are particularly well-fitted for delivering sensible heat from 120°C and above 500°C.

4. Conclusions

This paper investigates and compares R718 open cycle mechanical vapor compression (MVC) HTHP and Joule-Brayton (R729, R740, R744) HTHP with centrifugal compressors and turboexpanders. The results from the developed thermodynamic models lead to the following conclusions:

- There is a strong coupling between turbomachinery operating limits and the maximum deliverable heat temperature in HTHPs. For MVC HTHP, three-stage R718 centrifugal compressors are required to achieve condensation temperatures of 360°C with a high superheating of 500 °C at the compressor outlet. For Joule-Brayton HTHP, temperatures of 500°C are achievable with single-stage R729, R740, and R744 centrifugal compressors. The highest temperature lifts (above 700 K) achievable with a single-stage centrifugal compressor are with R740.
- For the highest possible temperature lift (240 K), MVC achieves a COP above 1.5. However, if the heat for liquid water heating is considered the adjusted COP is above 2. For lower temperature lifts (30 K) high COP can be obtained (10).
- Similar COP values of up to 2.2 are obtained for R729, R740, and R744 Joule-Brayton HTHPs for high temperature of generated heat (150-500°C). An increase in COP is observed when the compressor inlet pressure is increased to 80 bar for R744.

The MVC HTHP is recommended for steam generation and applications when the waste heat source is low pressure steam. The Joule-Brayton HTHP is recommended if sensible heat is required with a large temperature rise of the process heat carrier and a large temperature drop of the waste heat carrier.

Nomenclature

COP	coefficient of performance	(–)
h	specific enthalpy	(J kg^{-1})
l	specific compression work	(J kg^{-1})
p	pressure	(Pa)
s	specific entropy	(J $kg^{-1}K^{-1}$)
T	temperature	(°C, K)

x	liquid fraction	(kg kg^{-1})
T_c	condensation temperature	(°C, K)
T_e	evaporation temperature	(°C, K)
T_1	compressor inlet temperature	(°C, K)
η	compressor efficiency	(–)
Π	compressor pressure ratio	(–)

Acknowledgements

This research is conducted within the EIGEN (Energy Hubs voor Inpassing van Grootschalige Hernieuwbare Energie) project, subsidised by the Netherlands Enterprise Agency, Dutch Ministry EZK, Netherlands, under Grant Number MOOI 52101.

References

[1] Jiang J, Hu B, Wang RZ, Deng N, Cao F, Wang C-C. A review and perspective on industry high-temperature heat pumps. Renewable and Sustainable Energy Reviews 2022;161:112106. https://doi.org/10.1016/j.rser.2022.112106.

[2] Šarevski MN, Šarevski VN. Thermal characteristics of high-temperature R718 heat pumps with turbo compressor thermal vapor recompression. Applied Thermal Engineering 2017;117:355–65. https://doi.org/10.1016/j.applthermaleng.2017.02.035.

[3] Oehler J, Tran AP, Stathopoulos P. Simulation of a Safe Start-Up Maneuver for a Brayton Heat Pump. Volume 4: Cycle Innovations; Cycle Innovations: Energy Storage, Rotterdam, Netherlands: American Society of Mechanical Engineers; 2022, p. V004T06A003. https://doi.org/10.1115/GT2022-79399.

[4] Walden JVM, Bähr M, Glade A, Gollasch J, Tran AP, Lorenz T. Nonlinear operational optimization of an industrial power-to-heat system with a high temperature heat pump, a thermal energy storage and wind energy. Applied Energy 2023;344:121247. https://doi.org/10.1016/j.apenergy.2023.121247.

[5] Sharevska M, Sharevska M, Brem G, Hoogsteen G, Hurink J, Hajimolana Y. Systematic integration of high temperature heat pumps in industrial multi-energy systems. Applied Thermal Engineering 2025;278:127440. https://doi.org/10.1016/j.applthermaleng.2025.127440.

[6] Sharevska M, Sharevska M, Brem G, Hoogsteen G, Hurink J, Pozarlik A, et al. Comprehensive study of high temperature heat pump configurations: A framework of performance and application. Energy 2025;334:137525. https://doi.org/10.1016/j.energy.2025.137525.

[7] Šarevski MN. Influence of the new refrigerant thermodynamic properties on some refrigerating turbocompressor characteristics. International Journal of Refrigeration 1996;19:382–9. https://doi.org/10.1016/S0140-7007(96)80111-3.

[8] Sarevski MN, Sarevski VN. Water (R718) turbo compressor and ejector refrigeration/heat pump technology. Amsterdam Heidelberg: Butterworth-Heinemann; 2016.

[9] Higashimori H, Morishita S, Suzuki M, Suita T. Detailed Flow Study of Mach Number 1.6 High Transonic Flow in a Pressure Ratio 11 Centrifugal Compressor Impeller: Part 2 — Effect of the Inducer Shroud Bleed and Development of a Low Energy Region Along the Shroud, American Society of Mechanical Engineers Digital Collection; 2009, p. 1071–80. https://doi.org/10.1115/GT2007-27694.

[10] El Samad T, Żabnieńska-Góra A, Jouhara H, Sayma AI. A review of compressors for high temperature heat pumps. Thermal Science and Engineering Progress 2024;51:102603. https://doi.org/10.1016/j.tsep.2024.102603.

[11] Uusitalo A, Jaatinen-Värri A, Turunen-Saaresti T, Honkatukia J, Tiainen J. Centrifugal compressor design and cycle analysis of large-scale high temperature heat pumps using hydrocarbons. Applied Thermal Engineering 2024;247:123035. https://doi.org/10.1016/j.applthermaleng.2024.123035.

[12] Bergamini R, Jensen JK, Elmegaard B. Thermodynamic competitiveness of high temperature vapor compression heat pumps for boiler substitution. Energy 2019;182:110–21. https://doi.org/10.1016/j.energy.2019.05.187.

[13] Frate GF, Ferrari L, Desideri U. Analysis of suitability ranges of high temperature heat pump working fluids. Applied Thermal Engineering 2019;150:628–40. https://doi.org/10.1016/j.applthermaleng.2019.01.034.

[14] Zühlsdorf B, Bühler F, Bantle M, Elmegaard B. Analysis of technologies and potentials for heat pump-based process heat supply above 150 °C. Energy Conversion and Management: X 2019;2:100011. https://doi.org/10.1016/j.ecmx.2019.100011.